

Electronic Supplementary Information

Identification of Intracellular Gold Nanoparticles Using Surface-enhanced Raman Scattering

Hai-nan Xie,^a Yiyang Lin,^a Manuel Mazo,^a Ciro Chiappini,^a Ana Sánchez-Iglesias,^b Luis M. Liz-Marzán,^{bc} and Molly M. Stevens^{a*}

^a Department of Materials, Department of Bioengineering and Institute for Biomedical Engineering, Imperial College London, London SW7 2AZ, UK E-mail: m.stevens@imperial.ac.uk (M. M. Stevens).

^b BioNanoPlasmonics Laboratory, CIC biomaGUNE, Paseo de Miramón 182, 20009 Donostia - San Sebastián, Spain.

^c Ikerbasque, Basque Foundation for Science, 48011 Bilbao, Spain

Experimental

Chemicals

Polyvinylpyrrolidone (PVP) (MW~10,000), tetrachloroauric acid ($\text{HAuCl}_4 \cdot 3\text{H}_2\text{O}$), cysteamine, and N-(3-dimethylaminopropyl)-N'-ethylcarbodiimide hydrochloride (EDC), Triton X-100 were supplied by Sigma-Aldrich. NHS modified Alexa-750 and cell culture reagents were purchased from Invitrogen.

Functionalization of Au nanostars

Au nanostars were synthesized as described in a previously published paper.¹ Briefly, PVP-coated gold seeds (15 nm diameter, $[\text{Au}] 9.29 \times 10^{-4} \text{M}$) in ethanol were added to a mixture of HAuCl_4 ($2.73 \times 10^{-4} \text{M}$) and PVP (monomer concentration: 10 mM) in DMF under rapid stirring at room temperature. Within 20 minutes, the color of the solution changed from pink to blue, indicating the formation of gold nanostars. The prepared Au nanostars had an average size of $41 \pm 8 \text{ nm}$ in diameter, as determined from transmission electron micrographs. The synthesized nanostars were redispersed in 10 wt% PVP before further functionalization.

100 μL of 1 mM cysteamine were mixed with an equal amount of NHS-modified Alexa-750 overnight. 500 μL of 0.2 nM Au nanostar suspension was reacted with the cysteamine and NHS-modified Alexa-750 mixture for at least two hours. The whole suspension was then centrifuged and redispersed in $0.1 \times \text{PBS}$. The free amine sites on the unreacted cysteamine were blocked by carboxyl polyethylene glycol in the presence of 1 mg/mL EDC. The functionalized nanostars were redispersed in $1 \times \text{PBS}$ before the cell experiments.

Cell culture

HeLa cells were maintained in DMEM, 4500 mg/L Glucose supplemented with 10% v/v fetal bovine serum, 1% v/v L-glutamine and 1% v/v antibiotics. Upon confluence, cells were detached after a brief incubation in 0.05% v/v Trypsin, counted and plated on MgF_2 slides at a density of 10000 cells/ cm^2 .

The next day, media was changed for DMEM with 4500 mg/L Glucose without phenol red or serum supplementation, containing 1.2×10^{-11} M gold nanostars. 48 hours later, cells were gently washed in PBS with $\text{Ca}^{2+}/\text{Mg}^{2+}$, fixed in 10% v/v formalin (Sigma) for 15 minutes and washed again in PBS with $\text{Ca}^{2+}/\text{Mg}^{2+}$ before analysis.

Cell membrane destruction

Fixed HeLa cells on MgF_2 slides containing Alexa-750 functionalized gold nanostars were firstly immersed in 50 mM TCEP (dissolved in 1X PBS) for 1 hour. TCEP solution was initially replaced with 1% v/v Triton X-100. After 10 min, 1% v/v Triton was changed to 50 mM TCEP again for another 1 hour.

Characterization

Optical characterization was carried out by UV-Vis spectroscopy with Perkin Elmer Lambda 25. Fluorescence of the fluorophores was measured by Fluorolog from Horiba JOBIN YVON. The used excitation wavelengths for Alexa-750 and Cy5 were 720 nm and 620 nm, respectively. The concentrations of gold nanostars were identified through Nanosight LM10. TEM images were obtained with a JEOL 2100-F transmission electron microscope operating at an acceleration voltage of 200 kV. Samples for TEM were centrifuged at 5000 rpm and redispersed in ethanol several times to decrease PVP concentration. TEM images of cell slices were obtained after the Raman imaging following a protocol from Ref.14 in the main text.

SERS measurements

SERS mappings were performed using a Renishaw Invia system with a 785 nm line of a diode laser as the excitation source. The unfocused power output was measured to be ca. 0.5 mW at the sample. A Leica 63 \times /NA 0.9 water immersion objective was used for excitation and signal collection. The geometry of the scanned areas was 40 μm by 40 μm with step sizes of $1 \times 1 \mu\text{m}^2$. Dielectric edge filters were used to reject the Rayleigh scattered light. Spectra

were accumulated for 5 seconds and the scanning mode is streamline. For imaging the cell slices, the same parameters were used but with a 50× objective in air.

Solution SERS measurements were carried out on the same system but with a 10× objective.

The unfocused power output at the sample was ~1 mW for Alexa-750 and 50 mW for Cy5 with 1 s integration time.

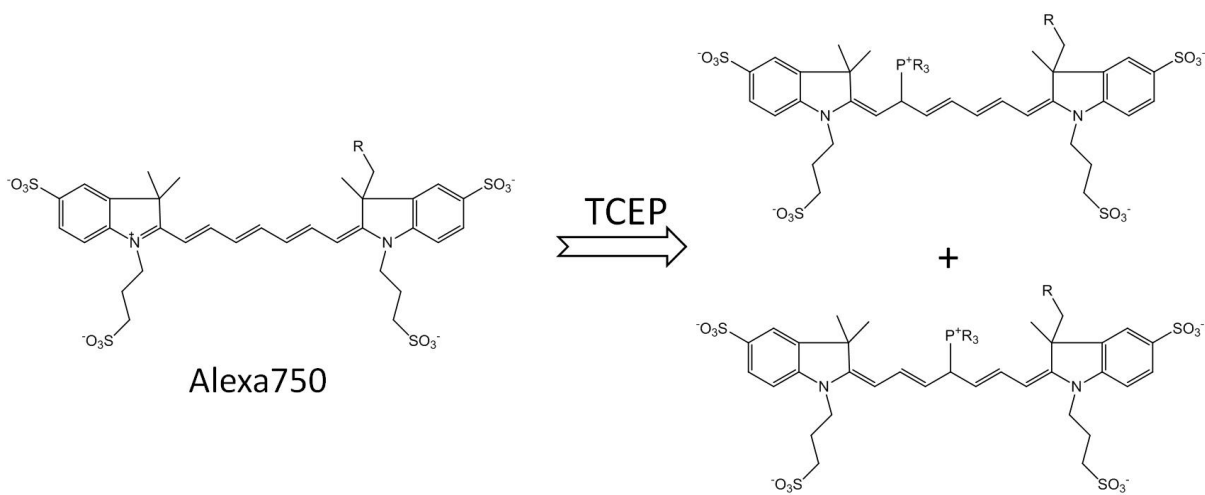
Discussion of the use of 785 nm laser excitation wavelength

Nanostars with their numerous tips generate a high density of hotspots and are therefore widely used for plasmon-assisted sensing. Near-field maps at the extinction maxima neatly illustrate the enhancement at the tips.² Once gold nanostars are aggregated, the use of longer wavelength excitation (>785 nm) may generate a stronger signal enhancement, because plasmon coupling will result in the red-shift of their localized surface plasmon resonance (LSPR). However, the creation of hot spots by aggregating gold nanoparticles will also generate a higher signal enhancement compared to the individual nanoparticles even if the laser excitation is not optimized.³ In addition, considering that the photon efficiency decreases as the excitation wavelength increases and Alexa-750 is resonant with a 785 nm excitation wavelength, employing a 785 nm laser is most appropriate for the experiments conducted here.

Calculation of the signal reduction using grey values and valid pixel areas:

Signal reduction

$$= \frac{\text{Grey value}_{TCEP(-)} \times \text{Valid pixel area}_{TCEP(-)} - \text{Grey value}_{TCEP(+)} \times \text{Valid pixel area}_{TCEP(+)}}{\text{Grey value}_{TCEP(-)} \times \text{Valid pixel area}_{TCEP(-)}}$$



Scheme S1. Possible addition reaction of Alexa-750 and TCEP. The mechanism of 1,4-addition of the phosphine to the polymethine bridge has been systematically studied by

Zhuang *et. al.*⁴

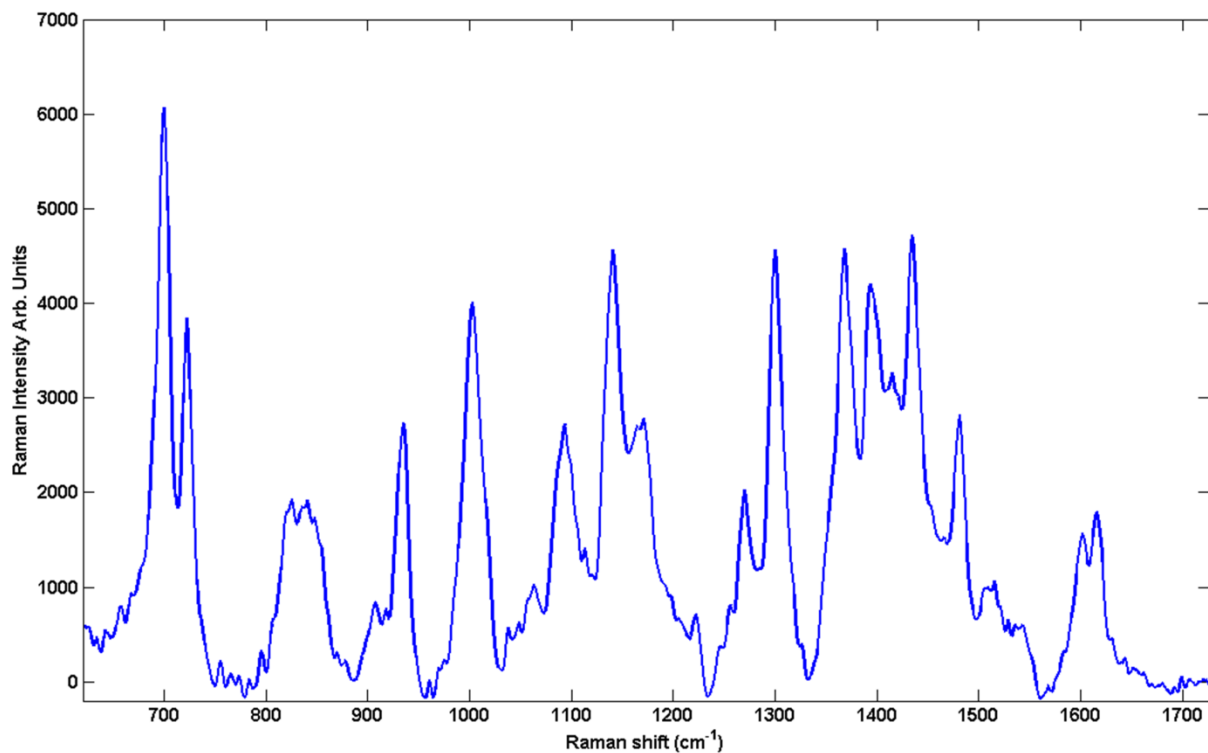


Figure S1. SERS spectrum of Alexa-750 adsorbed on gold nanostars at 785 nm excitation wavelength. The integration time was 1s, with ~1 mW power at the sample, the baseline was corrected with respect to the background.

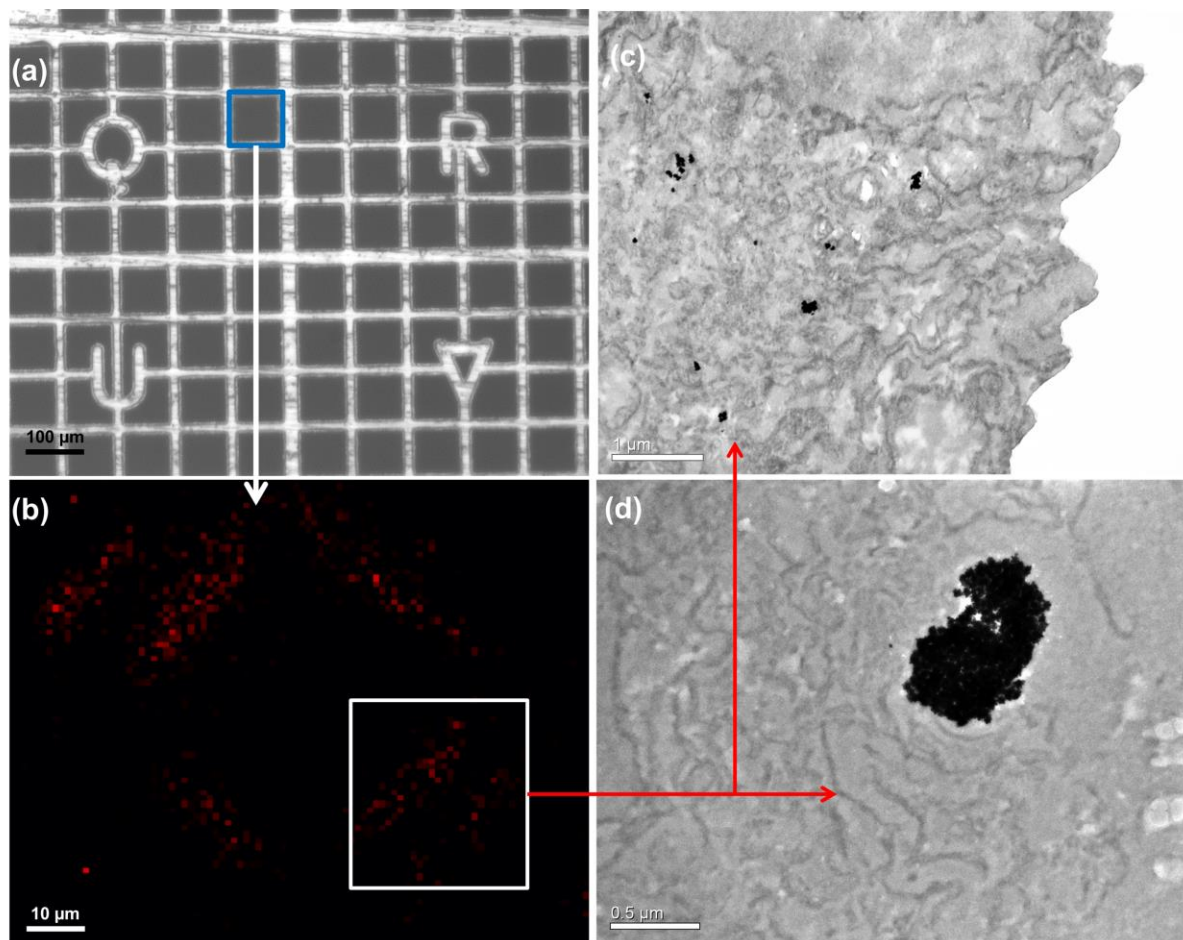


Figure S2. (a) White light image of an indexed TEM grid where the mapped area is indicated by a box; (b) Reconstructed SERS map of the cell slices on the grid based on the intensities of the highlighted peak in Figure 2c; 785 nm excitation wavelength, 10 second integration time, ~0.5 mW power at the sample; TEM grid itself does not generate any Raman signals under these conditions;. (c) and (d) Correlated TEM images of the cell slices from the same area.

Internalisation of gold nanostars by HeLa cells were observed from TEM images. No extracellular nanoparticles were observed possibly due to the intense washing steps during the sample preparations.

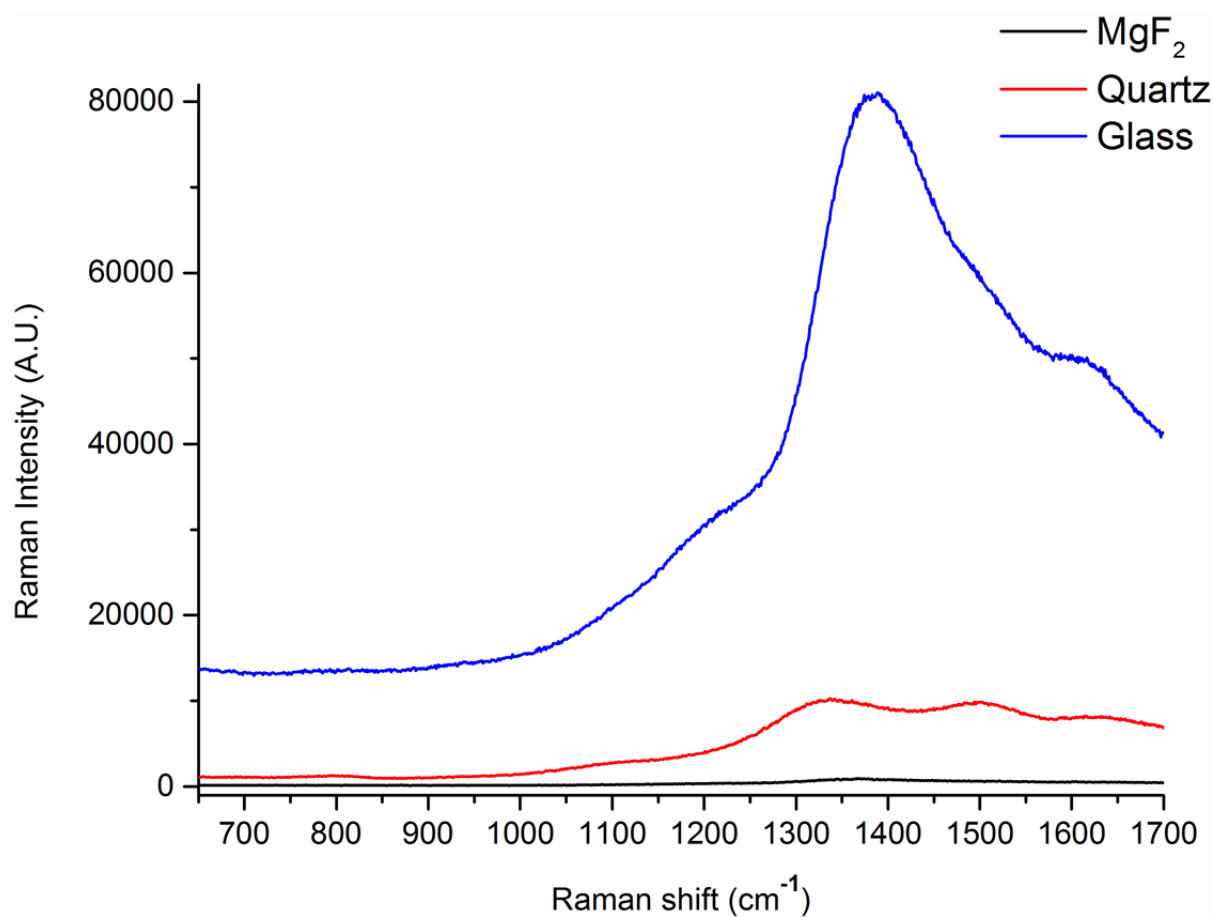


Figure S3. Raman background comparison among glass, quartz and MgF₂ slides at 785 nm excitation wavelength.

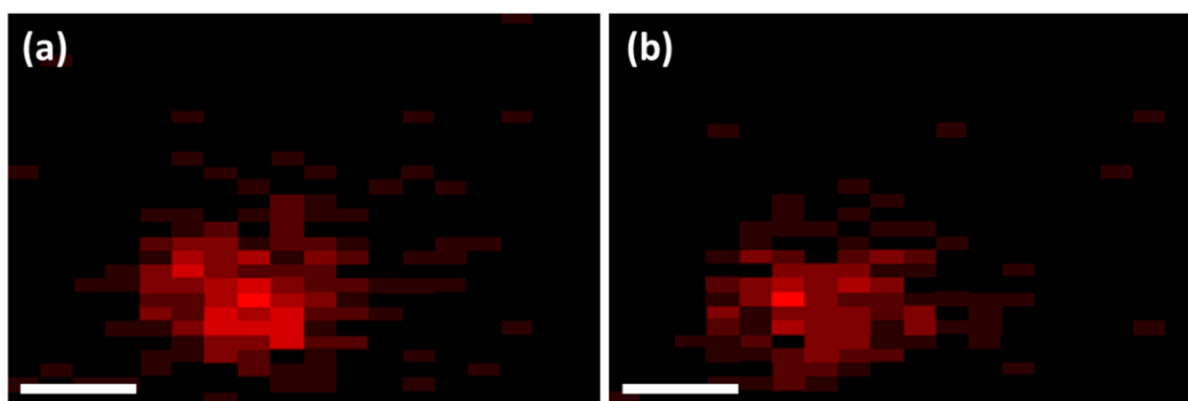


Figure S4. SERS maps of a HeLa cell from the first scan (a) and the second scan (b) of the same area. The signal reduction for the second time scan was ~9.8% based on their greyscale values and valid pixel areas. Scale bars are 5 μm.

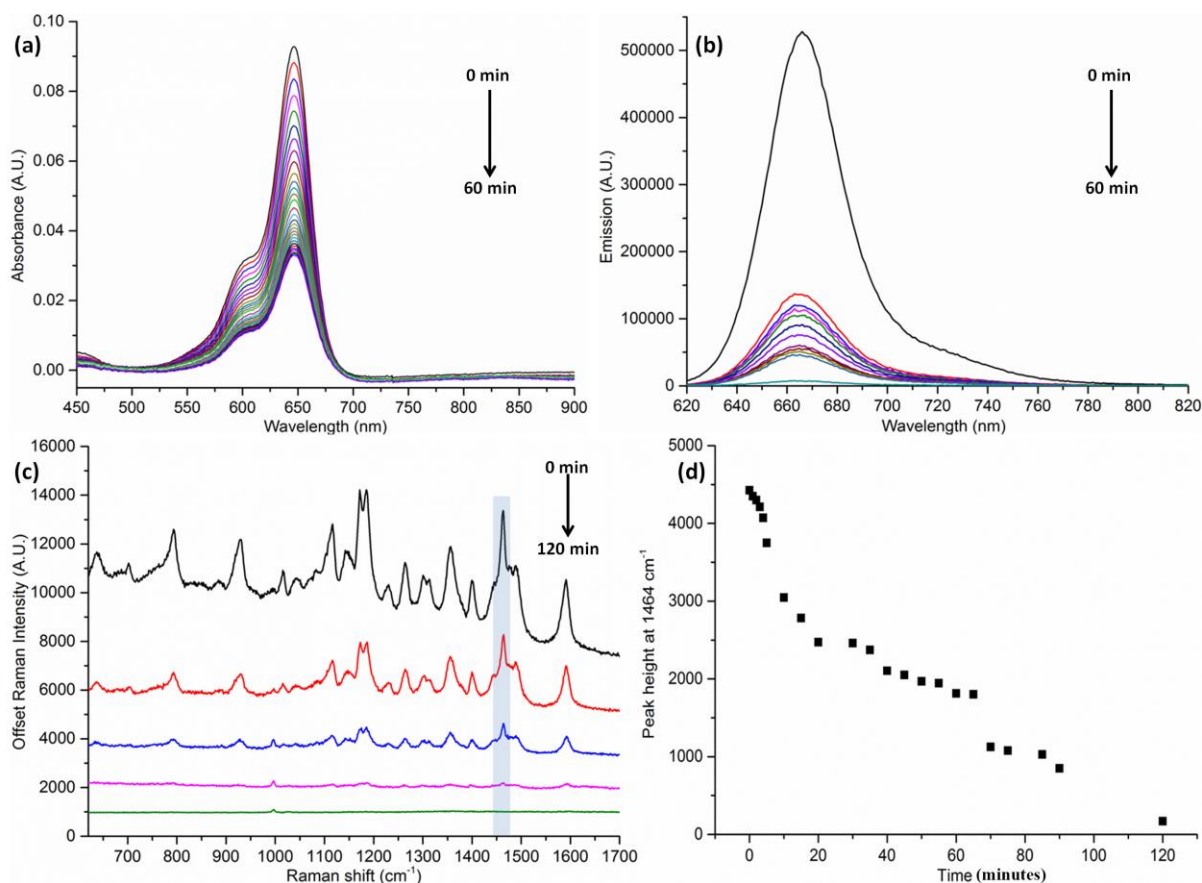


Figure S5. Absorption spectra (a) and emission spectra (b) of Cy5 after the addition of 10 mM TCEP; the excitation wavelength for emission was 620 nm. (c) SERS spectra of Cy5 after the addition of 50 mM TCEP. The excitation wavelength was 785 nm and the integration time was 1 second, with ~ 50 mW power at the sample. (d) Intensity of the highlighted peak in (c) versus time. In (a)-(c), the black lines correspond to the sample at time 0 min.

Reference:

1. P. S. Kumar, I. Pastoriza-Santos, B. Rodriguez-Gonzalez, F. J. Garcia de Abajo and L. M. Liz-Marzan, *Nanotechnology*, 2008, 19, 015606
2. D. M. Solís, J. M. Taboada, F. Obelleiro, L. M. Liz-Marzán, and F. J. García de Abajo, *ACS Nano* 2014, 8, 7559-7570
3. I. A. Larmour, E. A. Argueta, K. Faulds, and D. Graham, *J. Phys. Chem. C*, 2012, 116, 2677–2682
4. J. C. Vaughan, G. T. Dempsey, E. Sun and X. Zhuang, *J. Am. Chem. Soc.*, 2013, 135, 1197-1200.